Evolution of Nucleophilic High-molecular-weight Organic Compounds in Ambient Aerosols: a case study

Chen He[1], Hanxiong Che[2], Zier Bao[2], Yiliang Liu[2], Qing Li[2], Miao Hu[3], Jiawei Zhou[2], Shumin Zhang[4], Xiaojiang Yao[2], Quan Shi[1], Chunmao Chen[1], Yan Han[2], Lingshuo Meng[2], Xin Long[2], Fumo Yang[5]and Yang Chen[2*]

[1]State Key Laboratory of Heavy Oil Processing, China University of Petroleum, Beijing 102249, China.

[2]Research Center for Atmospheric Environment, Chongqing Institute of Green and Intelligent Technology, Chinese Academy of Sciences, Chongqing 400714, China.

[3] CNOOC Institute of Chemicals & Advanced Materials, Beijing 102200, China.

[4] Institute of Basic Medicine and Forensic Medicine, North Sichuan Medical College, Nanchong 637000, Sichuan, China.

[5] Department of Environmental Science and Engineering, College of Architecture and Environment, Sichuan University, Chengdu 610065, China

Correspondence to: Yang Chen (chenyang@cigit.ac.cn)

Abstract. Nucleophilic high-molecular-weight organic compounds (HMWOC) are sensitive to proton (H$^+$) in FT-ICR MS analysis. A comprehensive evaluation of diurnal evolution of nucleophilic HMWOC was performed. HMWOCs aged significantly in daily cycles, accompanied by functionality shifts, particularly oxygenated and reduced nitrogen (CHON and CHN), as well as oxygenated organics. The intensities of HMW oxygenated compounds increased during both daytime and nighttime. The daytime evolution produced more nitrogen-containing compounds with carboxylic groups (–COOH) homologs with molecular weights greater than 300, while the nighttime evolution produced mostly small CHON compounds (molecular weights <300). During evolution, nighttime CHON removals were observed; meanwhile, carboxylation was also identified in CHON groups. The daytime evolution produced significantly more reduced nitrogen-containing compounds; a day- and nighttime increase in CHN compounds with five members was also observed. This study can provide insights into the aging of less polar organic aerosols.

Keywords: high molecular weight organic aerosol; evolution; functionality

1 Introduction

Organic aerosol (OA) is a key component of atmospheric aerosols, accounting for up to 90% of submicron aerosols (Zhang et al., 2015; Tao et al., 2017; Zhang et al., 2007). OA affects solar radiation forcing, fog-cloud process, and human health (Pöschl, 2005; Creamean et al., 2014). The condensation of semivolatile vapors that are more oxidized onto primary OA can lead to the evolution of OA during their atmospheric lives (Jimenez et al., 2009), and the evolution can also be caused by heterogeneous processes in aerosol phase (Ervens et al., 2011).

OAs can undergo evolution during their lifetimes, resulting in changes in physicochemical properties (Ditto et al., 2021). The aged biomass burning emitted aerosols can be important sources of brown carbon (BrC) (Hodshire et al., 2019). During evolution, important components of Humic-like substances (HULIS), such as organosulfate and organonitrates, have been identified and observed in both laboratory and field measurements (Hallquist et al., 2009; Liggio and Li, 2006; Li et al., 2017b; Liu et al., 2015b). The heterogeneous reactions, such as acid–base reactions of amines/ ammonia with organic acids and carbonyls, can generate nitrogen- and oxygen- containing organics (Ervens et al., 2011; Zhang et al., 2015; George et al., 2015). The reduced nitrogen-containing compounds can be from the reactions of amines/ammonia and carbonyls (Zarzana et al., 2012; Liu et al., 2015b). These processings were important during long-range transport and severe haze formation due to stagnant air conditions in China (Li et al., 2017a).

The evolution of high-molecular-weight organic compounds (HMWOCs, M.W. larger than 200) is still an unsolved issue. For example, the overall oxidative state escalating was commonly observed, but how the oxidation and other processing occurred in HMWOCs. Most recently, online aerosol mass spectrometry has been widely used in evaluating OA, but the loss

of molecular information resulted in difficulties in investigating the aerosol HMWOCs (Zhang et al., 2011; Ditto et al., 2018). HMWOCs, commonly containing elements such as C, H, O, N, and S, can reach up to 1000 da in m.w. (Ervens et al., 2011). As a class of potentially light-absorbing components and precipitation participants, the environmental behavior of HMWOC is vital to

60   investigate to fully understand the impact of OA(Yun et al., 2019) (Bandowe and Meusel, 2017).

Fourier Transform Ion Cyclotron Resonance Mass Spectrometry (FT-ICR MS) is capable of extremely high mass accuracy and resolution for chemical analysis. It has been utilized extensively for characterizing complex organic mixtures of atmospheric OA (Xie et al., 2020; Jiang et al., 2014; Bianco et al., 2018). The method has been used to study HUMIC-like

65   substances, typically biomass burning and coal combustion aerosols (Li et al., 2022; Song et al., 2022; Tang et al., 2020; Laskin et al., 2014; Wang et al., 2019). FT-ICR-MS has been widely used in water-soluble organic carbon (WSOC) research using negative ion (–) electrospray ionization (ESI) mode. The (–)ESI mode has a good response on components in WSOC with functional groups of –OH and –COOH (Li et al., 2022; Zhang et al., 2021; He et al., 2022). Until

70   recently, HWM hydrophobic organic species, such as ester (ROR), hydrocarbons (C_xH_y), fatty acid, and reduced Nitrogen-containing compounds, were limitedly understood in ambient PM samples. CHN and CHON compounds are favorably detected in positive ion ESI ((+)ESI) mode compared to (–)ESI mode (Lin et al., 2012). This study will investigate the processing of HMW carbonyls, esters, amines, and other nitrogen-containing functional groups since they can form

75    $[M+H]^+$ ions in electrospray ionization operation positive ion mode (Kanawati et al., 2008; He et al., 2021a).

We present the molecular description of the diurnal evolution of HMWOCs that is sensitive to the (+) ESI mode in FT-ICRMS analysis to explore a wider context of HMWOC. In

this study, ambient $PM_{2.5}$ samples were collected for 5.5 hours for four samples in a daily cycle,

80   labelled as Morning, Afternoon, and Night, as well as midnight and early Morning (MEM) in an

urban area in Eastern China during spring for OA aging analysis. As a typical metropolitan area

in China, the sampling location is influenced by the local coal burning, biomass burning, traffic,

and residual emissions, as well as long-range transport. The molecular-level characterization of

HMWOC was explored, and organic subgroups' chemical composition and evolution under real-

85   world conditions were identified. This study can expand the understanding of HMWOC's

evolution in daily cycles and be supportive of evaluating the impact of organic aerosols.

2 Materials and Methods

2.1   Sample collection

The sampling site was located on the rooftop of a commercial building (119.0734° E,

90   33.6047°N) with a height of 45 m above the ground. The site is in a typical urban environment in

Huanan, Eastern China, with roads, parks, and residential areas nearby. Emissions from

restaurants, biomass, and coal burning from villages influence the region.

A high-volume sampler (Thermo Inc., USA) was used for $PM_{2.5}$ sampling at a flow rate

of 1.13 m^3 min^{-1}. $PM_{2.5}$ was collected using a quartz filter (Whatman Inc. USA). The filter was

95   pre-baked using a Muffle furnace at 600 °C to diminish organic species. Sampling periods are in

the midnight and early Morning (MEM) (23:00–4:30), Morning (5:00–10:30), Afternoon (11:00–

16:30), and Night (17:00–22:30). total of 52 samples were collected to describe the pattern of

$PM_{2.5}$ chemical composition, and samples from April 20th 2021 to April 21st, 2021 were selected

for FT-ICR MS analysis.

100   The routine PM$_{2.5}$ chemical composition was analyzed, including carbonaceous species,

water-soluble ions (SO$_4^-$, NO$_3^-$, NH$_4^+$, Cl$^-$, and Na$^+$), and elemental species. The protocols of

these analyses are available in the literature and *supportive information* (Wang et al., 2018). The

samples were punched from the quartz filter with an area of 0.526 cm^2. Then, the punches from

the same collection time were immersed using 10 ml acetonitrile with sonication for 10 min three

105   times. The acquired acetonitrile (ACN) solutions from the same sampling time were gathered,

combined, and concentrated to 1 ml for FT-ICR analysis.

2.2 FT-ICR MS analysis

The MS analysis of organic aerosol was carried out on a 7.0 T Bruker Solarix 2XR FT-

ICR mass spectrometer. The mixture of acetonitrile extract was vaporized to dry. Then, the dry

110   extract was reconstituted with water, and methanol was added proportionally in the water

solution before FT-ICR MS analysis. The samples at a concentration of about 50 mg/L were

dissolved in methanol for the ESI analysis. The samples were injected into the ionization source

at 120 µL/h through a syringe pump. The typical operating conditions for positive-ion ESI

analysis were: capillary voltage of –4.0 kV, capillary exit voltage of 200 V. Ions were

115   accumulated in the hexapole for 0.05 s then were transferred into the ICR cell with a time-of-

flight (ToF) of 0.7 ms. The ion transformation parameter for the quadrupole (Q1) was optimized

at *m/z* 200. The mass range was *m/z* 150–1000. A total of 128 scans with 4M data points were

accumulated to enhance the signal-to-noise ratio. Details of FT-ICR MS calibration and data

processing are provided in *Supportive information*. Briefly, FT-ICR MS was calibrated using a

120   reference list formed by the manually assigned known formula ($^{12}C_{0-100}$, $^{1}H_{0-200}$, $^{14}N_{0-10}$, $^{16}O_{0-20}$,

and $^{32}S_{0-2}$.) in Data Analysis.

2.3 FT-ICR MS data-related parameters integration

A modified aromatic index (AI_{mod}) and double bond equivalent (DBE) were calculated for each assigned formula, according to Koch and Dittmar. (2006). Kendrick mass defect (KMD) were calculated according to Stenson et al. (2003). The intensity-weighted average of elements (C, H, O, N, S), formulae (CHO, CHON, CHOS, CHONS), and other parameters (H/C, O/C, DBE, KMD, and AI_{mod}) were calculated for each sample. Molecular formulae were further assigned to the following groups as described by Seidel et al.(Seidel et al., 2014) and Antony et al(2015).

The OS_C is used to describe the composition of a complex mixture of organics undergoing oxidation processes. OS_C is calculated for assignable molecular formulae as follows (Kroll et al., 2011):

$$OS_C = -\sum_i OS_i \frac{n_i}{n_C}$$

Where OS_i is the oxidation state associated with the element I and n_i/n_C is the molar ratio of element I to carbon within the molecule. Other details of the data analysis are also available in *Supportive Information*.

When calculating OSc, the two elements, Nitrogen and Oxygen, were considered. In positive ESI mode, the valence of N was considered as -3. Also, S element was not considered because no S-containing molecules were detected in the sample in positive ESI mode.

3 Results and discussion

3.1 Overview of molecular characterization of organic aerosols

The overview of the sampling site is available in *Supportive Information*. The concentration-time profile is shown in Figure S1. Among all 52 samples, although the mass concentration of $PM_{2.5}$ showed a fluctuating trend in a range of 32–81 µg m^{-3}, the fraction of organic carbon was stable with a range of 0.18–0.21(Figure S1). During the sampling period, wind came from almost all directions, epically from north, south, east, and especially west at the daily level (Figures S2 and S3). Moreover, the meteorological parameters were also stable during the sampling. Therefore, we picked one of these days to evaluate the daily evolution of HMWOCs as the representative sample.

During the observation, the average concentrations of organic carbon (OC) were 12.8 µg m^{-3}, following an order of 12.7 µg m^{-3} (Night), 12.6 µg m^{-3} (Afternoon), 11.1 µg m^{-3} (Morning), and 9.4 µg m^{-3} (MEM). The concentrations of secondary organic carbon were also estimated as 5.1 µg/m^3 (46.0%), 5.0 µg/m^3 (39.3%), 5.6 µg/m^3 (43.8%), and 4.9µg/m^3 (51.6%), following order of Night≈ Morning> Afternoon >MEM.

A summary of acquired parameters for four samples from FT-ICR MS is shown in Table 1, and the samples are marked with MEM, Morning, Afternoon, and Night. Among four samples, the number of formulas between 5781 and 6566 was detected, with an order of Morning<MEM<Afternoon<Night. The average molecular weights of all four samples were: Morning (393 Da)< Afternoon (395 Da)<MEM (402 Da)< Night (406 Da). The relative intensity weighted element ratios, such as O/C$_w$ and H/C$_w$, were highest at Night, with values of 0.13 and 0.80, respectively, suggesting higher oxidation and saturation levels at Night compared to other

three stages. The relative intensity weighted carbon-normalized DBE (DBE/C_w) was the lowest at Night (0.21), also suggesting a high saturation level of organic compounds, possibly due to

165   primary emissions of OA.

The reconstructed (+) ESI FT-ICRMS mass spectra of four samples are shown in Figure 1. Most organic compounds were found M.W. between 200 and 400 Da. All the compounds in the organic aerosol are clustered into oxygenates (CHO) compounds, oxygen- and nitrogen-containing (CHON) compounds, and reduced nitrogen-containing (CHN) groups. No sulfur-

170   containing compounds were detected in the(+) ESI mode. On an intensity basis, the CHON is the largest subgroup, followed by CHO and CHN subgroups. CHON group accounted for 73% of the relative intensity in the MEM, and increased to 77%, 81%, and 93% in the Morning, daytime, and Night. CHN decreased from 10% to 3% after sunset. The result implies that daytime photooxidation significantly affected the chemical nature of HWOCs. In the following results

175   and discussion, a detailed analysis would perform for the nature of daily HMWOC aging.
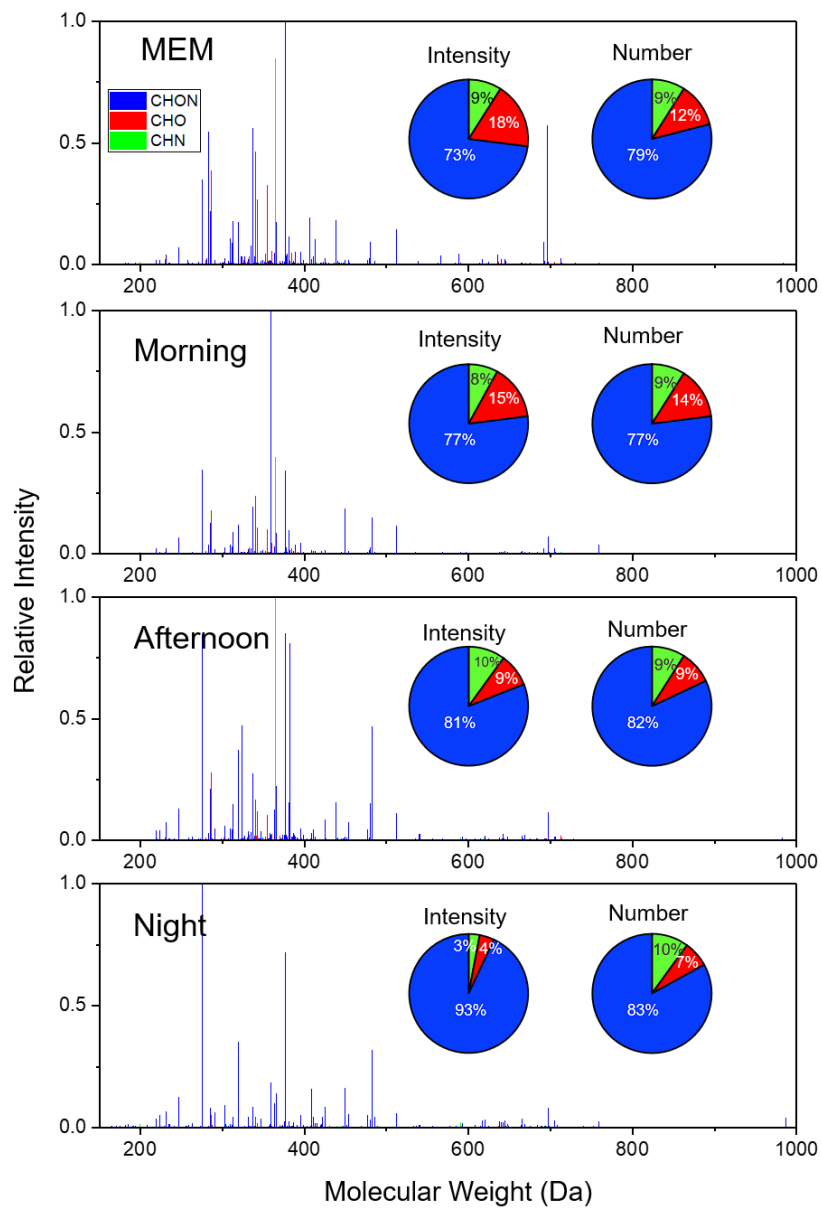
Figure 1. Mass spectra and distribution of relative intensity and formula number of CHON, CHO, and CHN compounds detected by positive-ion ESI FT-ICR MS.

180 **Table 1. Summary of molecular parameters of FT-ICRMS results among four samples during the different**

181 **periods.**

		Number Frequency	Molecular Weight (Da)	O/C_w	H/C_w	DBE	DBE/C
Midnight and Early Morning	All	5859	402	0.12	1.69	6.01	0.26
	CHO	715	345	0.13	1.47	6.88	0.31
	CHN	502	385	0	1.3	11.69	0.53
	CHON	4642	418	0.14	1.79	5.08	0.21
Morning	All	5781	393	0.12	1.66	6.35	0.26
	CHO	785	348	0.13	1.48	6.92	0.31
	CHN	531	482	0	1.43	12.23	0.41
	CHON	4465	402	0.13	1.74	5.66	0.23
Afternoon	All	6376	395	0.12	1.75	5.74	0.25
	CHO	606	368	0.13	1.47	7.03	0.31
	CHN	565	385	0	1.29	11.65	0.53
	CHON	5205	399	0.13	1.84	4.84	0.21
Night	All	6566	406	0.13	1.8	5.13	0.21
	CHO	432	429	0.12	1.46	8.22	0.31
	CHN	648	416	0	1.51	9.12	0.37
	CHON	5486	405	0.14	1.82	4.88	0.2

182

3.2 Evolution of CHO compounds and functionality

185   In the (+) ESI mode, the CHO group is favorably detected as carbonyl and ester compounds, but we can not simply assign those compounds as carbonyl and ester compounds because it was highly likely to contain -COOH or -OH in one molecule. (Ditto et al., 2021). In number frequency, CHO increased from 12% (MEM) to 14% (Morning), then decreased to 7% until the Night. CHO molecules contained up to ten oxygen atoms, but most of the CHO compounds with an oxygen atom number ≤ 4,

190 such as 74.7% in MEM, 73.5% in Morning, 69.5% in Afternoon, and 72.2% in Night.

    As shown in Figure 2, a classification was performed based on the iteration of *Antony et al.* (2014). We used Van Krevelen diagrams and the criteria from Antoy et al. (2014). The classification of Saturated hydrocarbons, unsaturated hydrocarbons, lipids, lignin, and polyphenols is only used as a reference for a better understanding of the distribution of organic molecules and the corresponding

195 environmental impacts. The saturated hydrocarbons, including lipids, alkanes, and aliphatics, were dominated, and they were mainly from traffic (Zhang et al., 2011), biogenic emissions, or biomass burning (Chen et al., 2014), alcohol synthesis(Ao et al., 2018), and biofuels (Rice et al., 2019). In a number frequency view, unsaturated hydrocarbons were 1.2 times more in MEM sample than in Morning, 1.3 times more than in Afternoon, and ~ 1 time in Night. Both samples' frequency was

200 promoted by traffic emissions but removed by daytime photochemical activities (Mcguire et al., 2014).
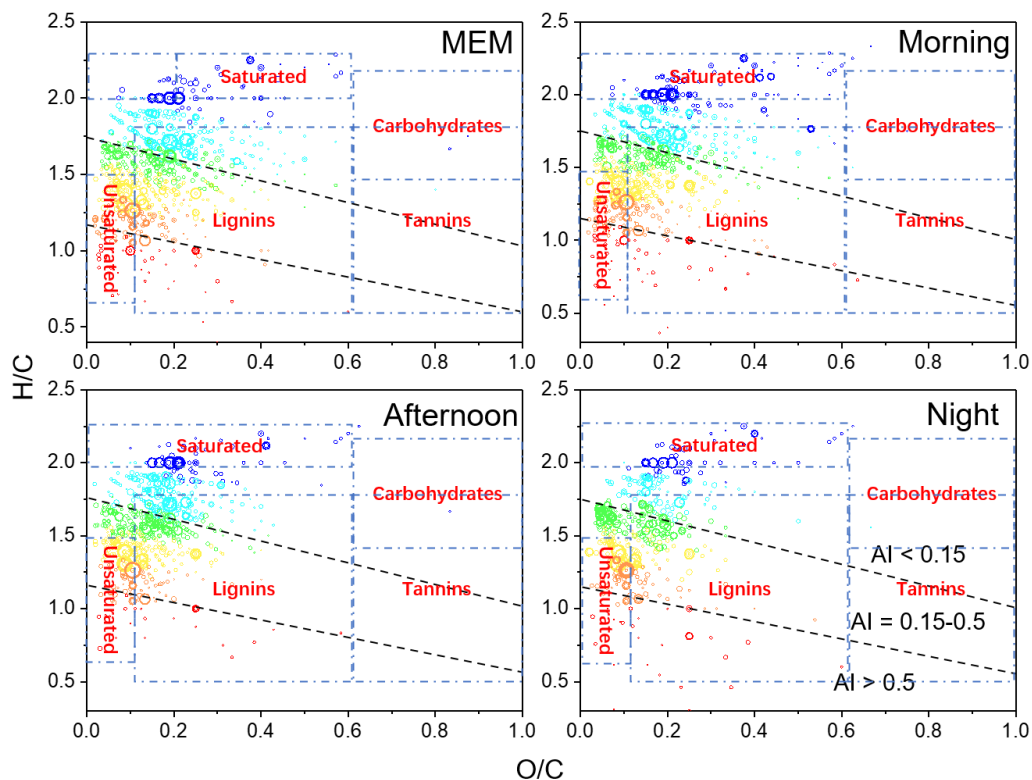
Figure 2. Van Krevelen diagrams (H/C vs. O/C ratio) for CHO species with various aromatic index (AI) value ranges. The dashed lines separate the different AI regions. The size of the symbols reflects the relative peak intensities of molecular formulae on a logarithmic scale.

205   Figure 3 illustrates the DBE against carbon number with color bars denoting the numbers of oxygen. The CHO compounds showed the highest DBE up to 26. Among them, CHO compounds with oxygen atoms ≤ 4, carbon atoms ≤ 25, and DBE between 4 and 16 were favorable phenol compounds with one or two aromatic rings (Yu et al., 2016). However, the HMW CHOs with carbon atoms ≥ 25 were commonly with oxygen atoms ≥ 6. They were recognized as HUMIC-like substances that were

210   abundant with –OH, –COOH, and –CHO but an absence of nitrogen (Kurek et al., 2020). Figure S5

implies that the highest carbon oxidation state (OSc) occurred in compounds with a number of carbon atoms around 15.
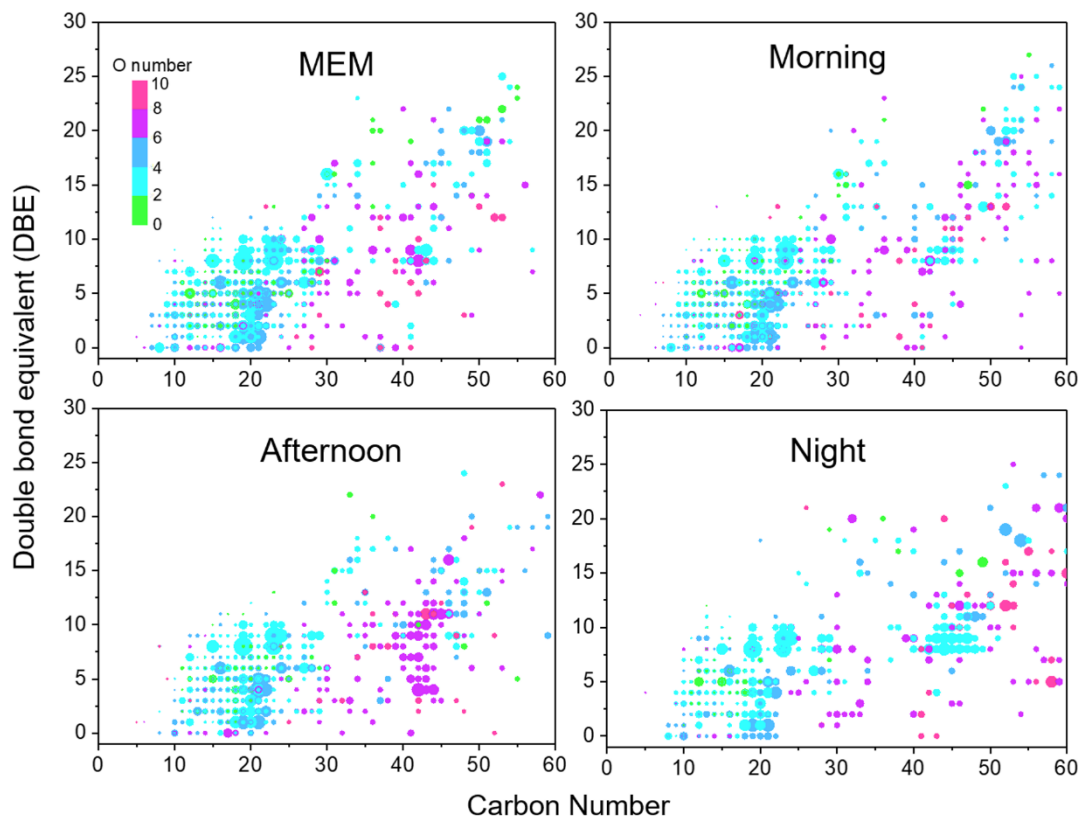
Figure 3. Carbon number vs. double bond equivalent (DBE) for CHO species. The color bar denotes the number of O
215   **atoms. The size of the symbols reflects the relative peak intensities of molecular formulae on a logarithmic scale.**

The daytime photochemical activities extremely change the functionality of CHO compounds. For example, CHO with 20 carbon atoms was observed with more oxygen atoms in Morning and Afternoon samples than that in MEM and Night. Particularly, CHO compounds with carbon numbers between 40 and 50 were prominent in Afternoon, possibly due to the formation of –C=O and –COO via

daytime photochemical reactions. Then, at Night, organic compound containing more oxygen atoms were found (O number >6, DBE>5 and carbon atoms >50) were found appeared in the nighttime. Meanwhile, The batch of primary OA and less-oxidized SOA was also observed, such as CHO compounds with carbon atoms between 45–50, DBE between 5–10, and O atoms between 0 and 2. In addition, after serious aging, the highly oxidized CHO compounds with oxygen atoms larger than eight significantly increased in Night and MEM samples (Huang et al., 2014).

As shown in Figure 4, the KMD analysis of CHO compounds was performed. Many homologues of CHO compounds are present as the "core" molecules plus $(CO)_n$ (n= 0,1, 2, 3, …) as a result of carbonyl formation. Among these CHO homologs with KMD_{CO} between 0.4 and 0.0, and oxygen atoms less or equal to four, carbonyl was favorably resistant or produced in the Morning vs. MEM scenario. However, in the Afternoon vs. Morning scenario (Figure 4b), as well as Night vs. Afternoon scenario (Figure 4c), the removal of carbonyls exited among CHO with oxygen atoms from one to ten. Likewise, the formation of carboxylic acids (–COOH), represented by $(COO)_n$ homologs, were significantly formed in Morning and removed in both Afternoon and Night, suggesting continuing destruction of carboxylic acids. Interestingly, the CHO compounds with oxygen numbers less or equal to two continued forming without solar radiation at Night. The removal of carbonyls could be attributed to further oxidation to carboxylic acids as well as reactions with H_2SO_4 and HNO_3 to create organosulfate and organonitrates, or reply with ammonia to form reduced nitrogen-containing compounds (Liu et al., 2015b) (Ervens et al., 2011).
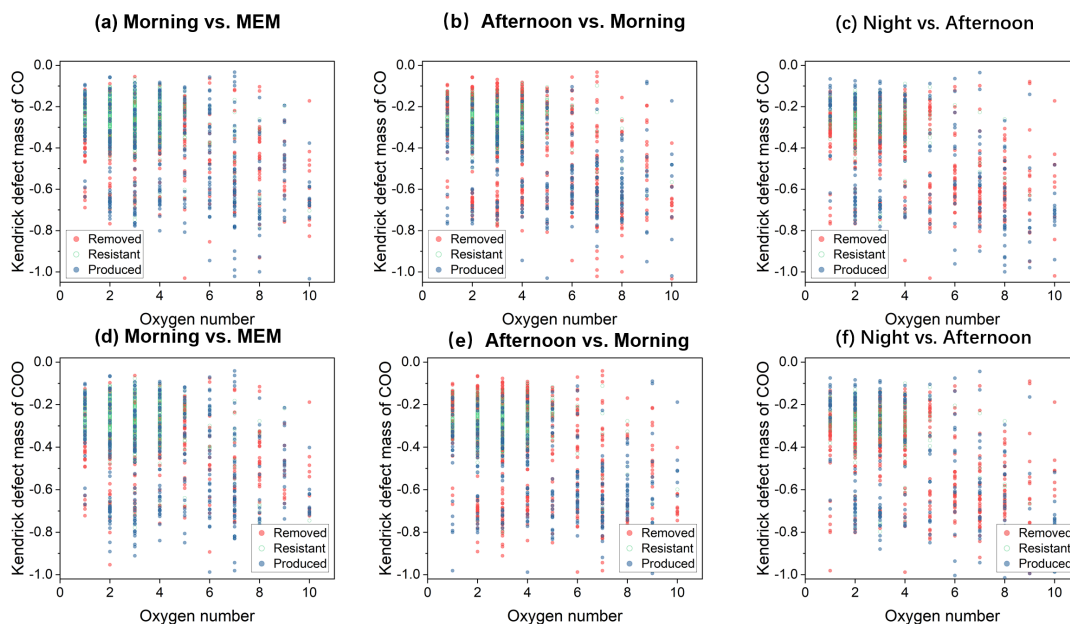
Figure 4. Kendrick Mass Defect (KMD) plots of CHO compounds in diurnal evolution of CO series (a, b, and c) and COO series (d, e, and f)

3.3 Evolution of CHON compounds and functionality

CHON compounds were the most abundant group in the (+)ESI results, accounting for 79%–83% in number frequency. The average molecular weight decreased during the daytime, from 418 Da in MEM to 402 in Morning, and 399 in Afternoon, then increased to 405 at Night. O/C_w varied from 0.13 to 0.14, while H/C_w was between 1.74 to 1.82. O/C_w was lower than 0.18, and H/C_w was higher than 1.5 (Table 1). The HMWOCs in the range of above parameters were likely from biomass burning, as reported in a previous study by Song et al., 2022.

As shown in Figure 5, most CHON compounds, accounting for 60%–63%, were with $H:C_w> 1.7$

and $AI< 0.15$. These CHONs were nitrogen-containing, and most were with $-NO2$ or $-ONO2$, namely

unsaturated organonitrate. The details of CHON compounds with higher O/N ratios ($\geqslant 3$) are discussed

in the following text. The unsaturated organonitrates were more pronounced in both MEM and

Afternoon, taking up to 63.2% and 63.3%, respectively. The highly unsaturated ($H:C=0.7-1.5$ and

$0.15<AI<0.5$) decreased from 33.8% in Morning to 21.6% in Afternoon, possibly due to the influence

of photobleaching from daytime photochemical activities(He et al., 2021b). Also, the aromatic CHON

($AI>0.5$) increased to 3.1% at Night.
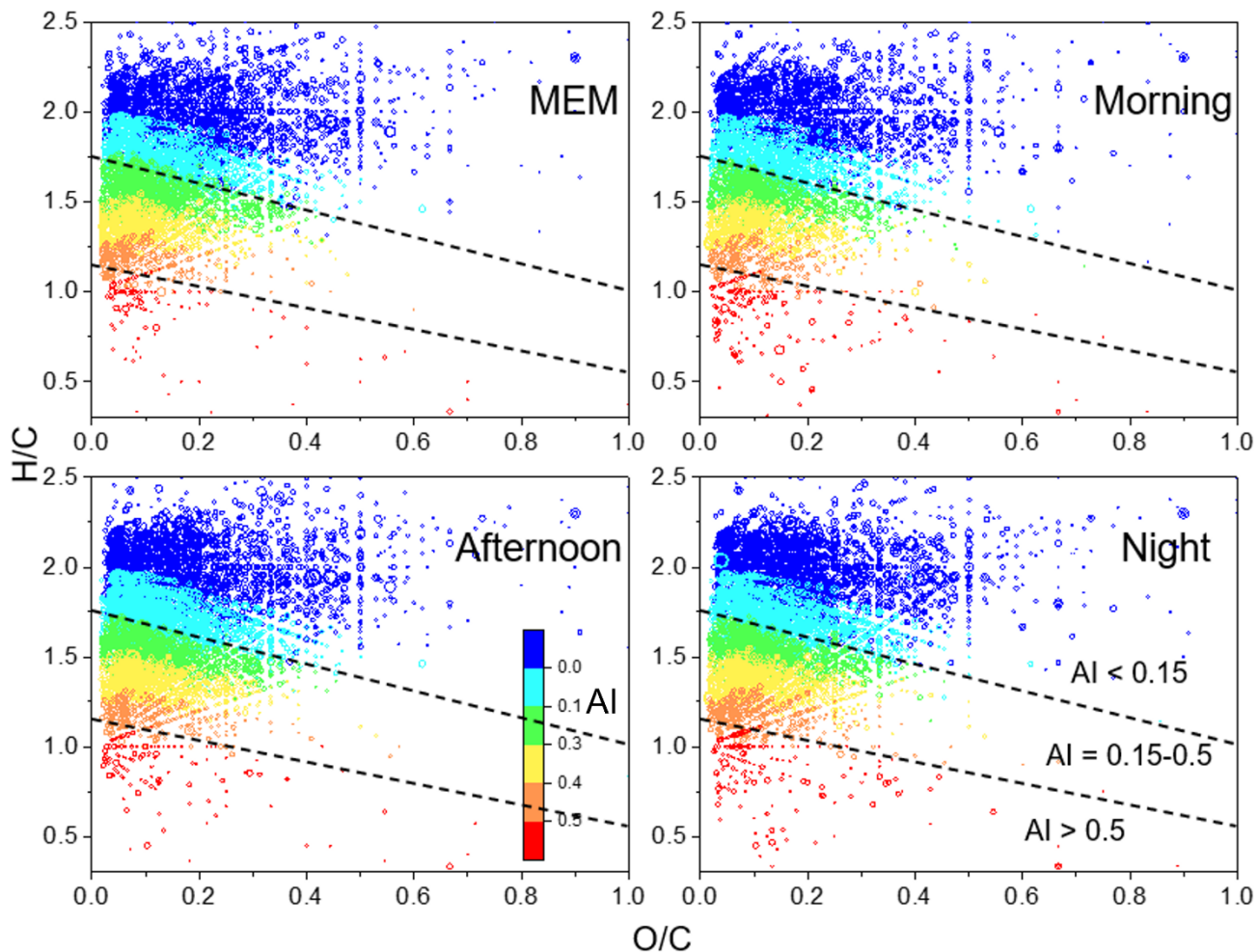
Figure 5. Van Krevelen diagrams (H/C vs. O/C ratio) for CHON species with various aromatic index (AI) value ranges. The dashed lines separate the different AI regions, and the color bar is AI values.

The OSc diagram against carbon number is shown in Figure 6. Most CHON compounds are distributed in a range of carbon numbers between 10 and 40 and OSc between –2 and 1. Those long-chain nitro-hydrocarbon with carbon numbers between 30 and 60 were substantially enhanced by the morning rush hours. During the daytime, CHON compounds with carbon numbers between ten and 30

and OSc between –1 and 0 were enhanced, suggesting that more aged nitro-hydrocarbons were

265   produced in the daytime.
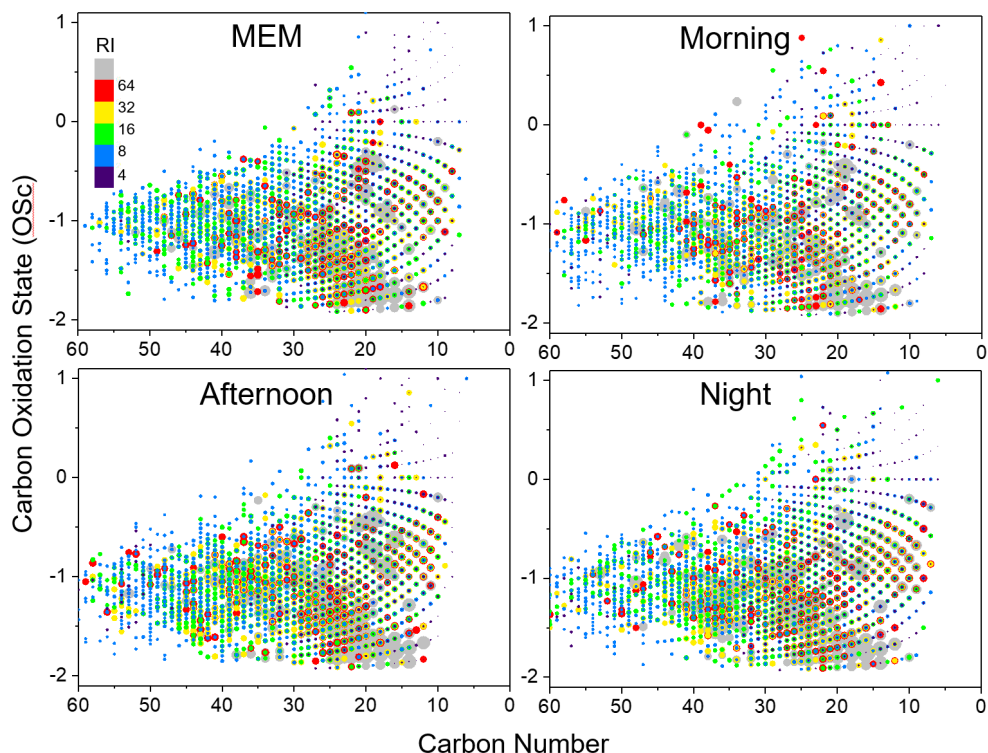
Figure 6. Overlaid carbon oxidation state (OSc) symbols for CHON species. The size and color bar of the markers reflects the relative peak intensities of molecular formulae on a logarithmic scale. RI: relative intensity.

270   Typically, CHON compounds with higher O/N ratios (≥ 3) can be attributed to organic nitrate

($RONO_2$) groups in +ESI mode (Song et al., 2022). The organonitrates accounted for 21.9%−24.0% of

CHON compounds, and the associated ratios of log RI were between 22.2%−23.0%. $RONO_2$

compounds were more prominent in the Morning (24.0%), and lower without sunlight (e.g., 21.9% in

MEM). RONO$_2$ compounds with AI>0.5, attributed to polycyclic phenolic compounds, escalated in the

275 Morning (from 1.7% to 2.1 % after the rush hour), then decreased to 1.9% in Afternoon, and then

increased to 2.0% at Night.

As shown in Figure S6, N$_1$O$_x$ (x=1–9) with DBE< 5 were the most abundant in the CHON

subgroup, accounting for 49%–51% of CHON compounds in number frequency. Since most CHON

compounds contained only one nitrogen atom, the CHON$_1$ group was chosen for further evaluation.

280 Figure 7 shows that the CHON$_1$ CH$_2$-homologues with molecular mass between 150 and 400 were

stable as being resistant, as shown in Figure 7 a–c. However, CHON$_1$ compounds with M.W. smaller

than 200 were removed in Afternoon but produced in Night. The nighttime chemistry strongly removed

the CHON$_1$ CH$_2$-homologues with m.w.> 600 (Figure 7c). These results suggest the diversities of

atmospheric fate of CHON$_1$ compounds.
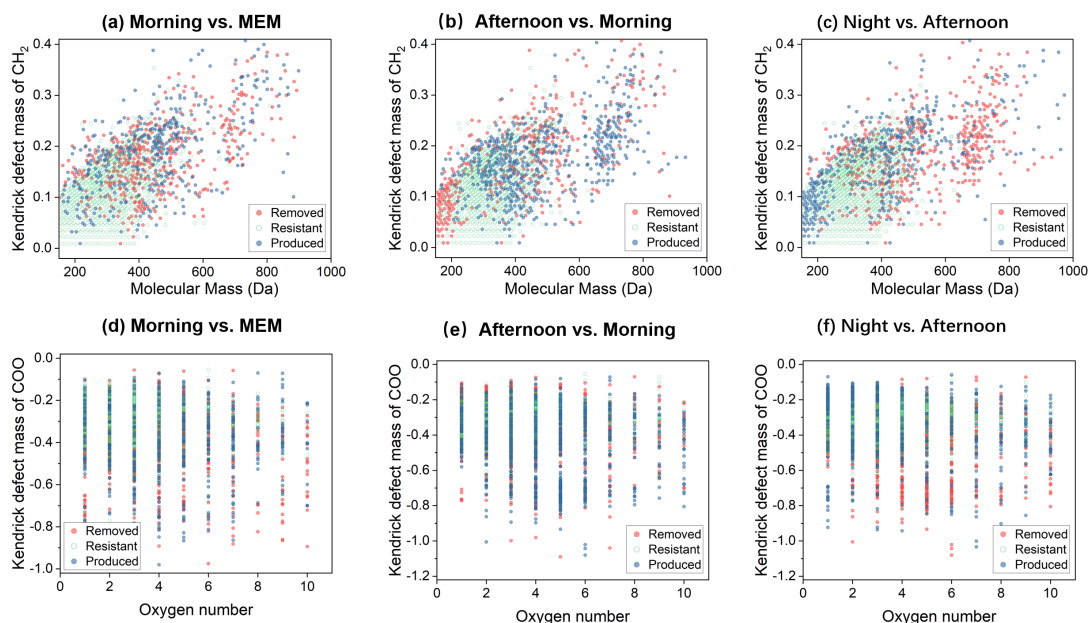
285

Figure 7. Kendrick mass defect (KMD) plots of CHON$_1$ compounds in diurnal evolution of CH$_2$ series (a, b, and c) and COO series (d,e, and f)

In an KMD view, as shown in Figure 7 (d–f), CHON$_1$ compounds (COO homologous) were removed in Morning, while produced prominently in Afternoon and Night (Figures 7(d) and 7(e)). Those results suggested that the organonitrates continued performing multi-generation oxidation to produce more carboxylic functional group (−COOH), and the carboxylic functional group can be due to the reaction with acids such as HNO$_3$ and H$_2$SO$_4$ to form organonitrate and organosulfates or be neutralized by NH$_3$ to form ammonium salt or reduced N-containing compounds in the particle phase (Lim et al., 2016; Darer et al., 2011; Zarzana et al., 2012). In previous studies, those processes were proven to occur in small carboxylic acids. In this work, we can observe a similar process on HMWOCs.

3.4 CHN compounds' evolution and functionality

CHN compounds remained stable in the FT-ICR dataset, accounting for 9%–10% in number and 3%–10% in intensity. The average H/C$_w$ was between 1.30 and 1.51 among four samples. As shown in the DBE against carbon number diagram (Figure 8), most CHN compounds have carbon numbers between 10 and 60, as well as nitrogen numbers from 1 to 10. Only a trivial proportion (3.0%–4.5%) of CHN compounds with DBE=0 and carbon numbers>10 as long-chain aliphatic amines (Song et al., 2022). Long-chain aliphatic amines could be emitted from traffic and biomass emissions in the Morning, then decrease to 3.0% in the Afternoon, and finally reach 4.5% at Night due to rising relative humidity (Chen et al., 2019).
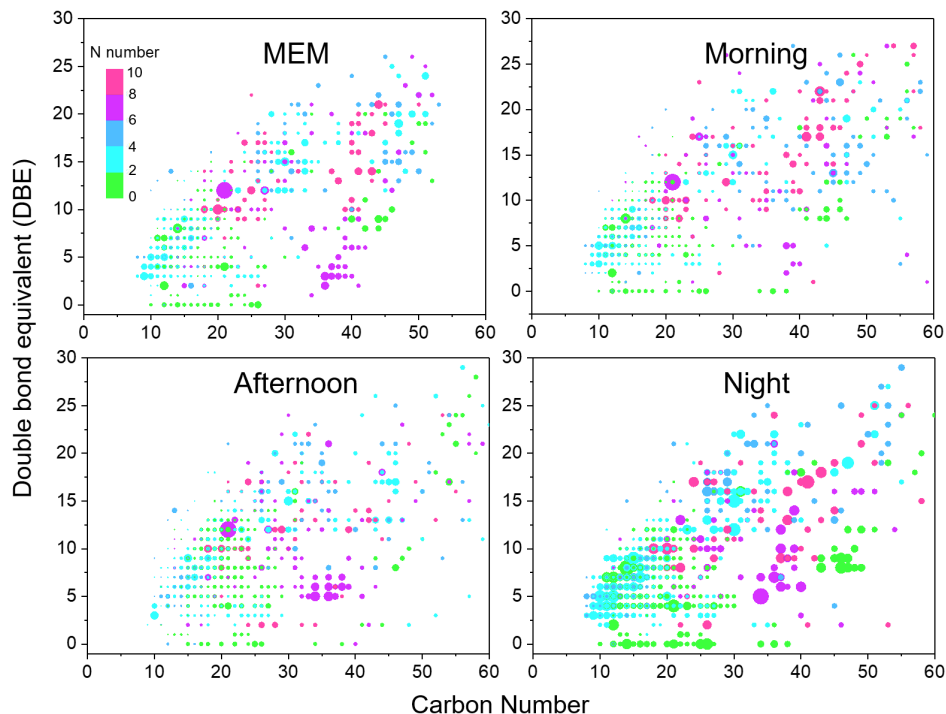
305

Figure 8. Carbon number vs. double bond equivalent (DBE) for CHN species. The color bar denotes the number of N atoms. The size of the symbols reflects the relative peak intensities of molecular formulae on a logarithmic scale.

CHN compounds with two nitrogen atoms (N_2) and DBE>5 were the most abundant group. For example, the series of $C_5H_8N_2(CH_2)_n$, $C_5H_6N_2(CH_2)_n$, and $C_7H_6N_2(CH_2)_n$ homologous series were likely

310 imidazole, pyrazine/pyrimidine, and azaindole homologous series, respectively (Wang et al., 2019). 16%–18% of N_2-containing CHN compounds attributed to five-membered rings such as pyrazole, imidazole, and their derivatives, or six-membered rings N-heterocyclic species . The abundance of N_2-containing CHN compounds showed an increasing trend from 16.3% (MEM) to 27.2% at Night.

The nitrogen number(N_n)>8 CHN compounds occurred in both day- and nighttime, suggesting

315   the impact of the secondary formation of CHN compounds. After diurnal processing, the relative

intensities of CHN compounds, with C numbers between 20 and 50, were enhanced (Figure 8). This

result was consistent with the KMD analysis, as shown in Figure 9.
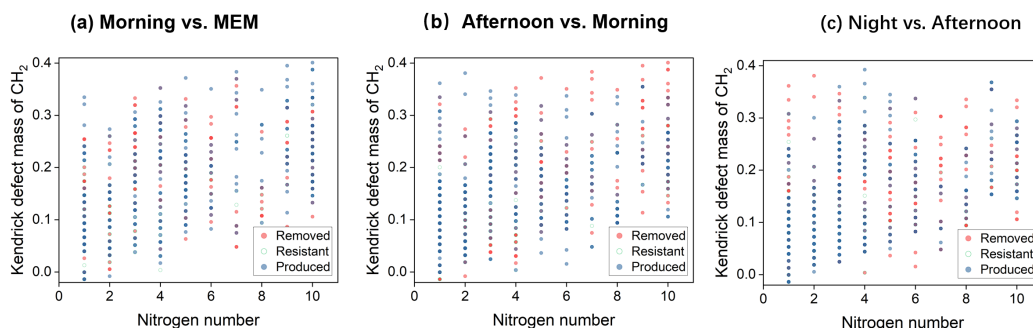
Figure 9. Kendrick mass defect (KMD) plots of CHN compounds in diurnal evolution of CH2 series (a, b, and c).

320   The $N_{8–10}$ containing CHN compounds accounted for 11.4%–18.5% among the four stages,

appearing with homologous series. They typically appeared with carbon numbers larger than 20, with

the largest abundance in MEM (18.5%). These CHN compounds can be vaporized from coal burning,

especially in the smoldering stages. Therefore, the $N_{8–10}$ containing CHN compounds were reasonably

more pronounced at low temperatures from residential coal use for heating. Besides the primary

325   emission, small CHN compounds can also form from the reactions between amines/ammonia and

carbonyl-containing SOA (Zarzana et al., 2012; Liu et al., 2015b). Our results suggested that the

formation of HMW CHN was also possible.

4   Atmospheric implications

Noticeable that there were some limits on this work. Under the variable emission, atmospheric process, and long-distance transport of organic aerosols, the samples can give a snapshot the evolution in the region, and the analysis can cause uncertainties. Therefore, this work can be treated as a case study. This study is an attempt to evaluate the evolution of high molecular weight organics using FT-ICR MS. Since the technique is a non-quantitative, and the matrix effect cannot be ignored. Those facts lead to considerable uncertainties. When discussing the evolution of HMWOCs, it is noticeable that the formation of higher oxidative groups such as carbonyl or carboxylic acid groups, commonly were accompanied with loss of other atoms such as hydrogen or even breaking up of the carbon chain. However, those process are difficult to be illustrated using FT-ICR MS method.

We present the molecular description of the diurnal evolution of HMWOCs that is sensitive to the (+) ESI mode in FT-ICRMS analysis to explore a wider context of HMWOC. The uptake of ammonia on biogenic or anthropogenic SOA to form light-absorbing nitrogen containing organics has been reported (Li et al., 2017b; Liu et al., 2015a). In this study, we proved that the nucleophilic oxygenated and nitrogen-containing compounds can also undergo substantial aging. Commonly, the nucleophilic HMWOC were considered less polar, and their evolution were different. We found more –CHO and –COOH groups were detected in the daytime for the CHO subgroup, and the aerosol-phase oxidation continued in the dark, resulting in more oxidized HMWOCs.

The formation of HMW organonitrates was also complicated. We have observed the prominence of organonitrates in both day and Night. In the daytime, the possible pathway includes the reactions of

NO_2 radicals with aliphatic hydrocarbons and aromatic rings. At nighttime, the adduct of NO_3 radical on HMWOC could possibly occur. In polluted urban areas, the rich nitrogen oxides (NO_x) environment

350 produced nitrate as well as organonitrates. The processing can shift the nitrogen deposition and be important on a local or regional scale. Also, the $CHON_1$ compounds were along with carboxylation, suggesting that the multiple oxidations of organonitrates can occur in both day- and nighttime. The process can enhance hygroscopic growth and CCN activities due to the acid-base reactions between ammonia and organics with carboxylic acids (Dinar et al., 2008).

355 The daytime CHN compounds could produce from the condensation reaction between –CHO groups and ammonium/amines. It might propose that the formation of long-chain CHN might be less important, however, those species have possibly five- or six-member rings that can act as chromophores. Along with the primary emission of HMW CHN from coal combustion and biomass burning (Brege et al., 2018; Ray et al., 2019), the sources of BrC should be reconsidered. Moreover, the

360 impact of ammonia was commonly on its potential impact on nitrogen deposition or forming the secondary in organic aerosol, but we suggest assessing its effect on the formation of HMW BrC. Conclusively, the evaluation of nucleophilic HMOC properties due to variability should be considered in future studies for improvement of air quality and climate model performances.

Data Availability

365 Data supporting this paper can be found at https://doi.org/10.5281/zenodo.7830299.

Author Contribution

YC designed this study. QL, CH, MH, and HChe contributed to the data collected during the field campaign. JZ, SZ, and YX performed field experiments. YL, XY, YH, XL, LM, QS, CC, FY and YC contributed to the scientific discussion and paper correction.

370 **Competing interests**

The contact author has declared that none of the authors has any competing interests.

Acknowledgments

The authors are grateful for the assistance of colleagues for sample collection.

Financial support

375   This research has been supported by the National Natural Science Foundation of China (grant no. 42075109, 42275126 and 42107452), and the Science Foundation of China University of Petroleum, Beijing (2462023YJRC003).

References

Antony, R., Grannas, A. M., Willoughby, A. S., Sleighter, R. L., Thamban, M., and Hatcher, P. G.: Origin and sources of
380   dissolved organic matter in snow on the East Antarctic ice sheet, Environ. Sci. Technol., 48, 6151-6159, 10.1021/es405246a, 2014.

Ao, M., Pham, G. H., Sunarso, J., Tade, M. O., and Liu, S.: Active centers of catalysts for higher alcohol synthesis from syngas: a review, Acs. Catalysis., 8, 7025-7050, 2018.

Bandowe, B. A. M. and Meusel, H.: Nitrated polycyclic aromatic hydrocarbons (nitro-PAHs) in the environment - A review,
385   Sci. Total. Environ., 581-582, 237-257, 10.1016/j.scitotenv.2016.12.115, 2017.

Bianco, A., Deguillaume, L., Vaitilingom, M., Nicol, E., Baray, J. L., Chaumerliac, N., and Bridoux, M.: Molecular Characterization of Cloud Water Samples Collected at the Puy de Dome (France) by Fourier Transform Ion Cyclotron Resonance Mass Spectrometry, Environ Sci Technol, 52, 10275-10285, 10.1021/acs.est.8b01964, 2018.

Brege, M., Paglione, M., Gilardoni, S., Decesari, S., Facchini, M. C., and Mazzoleni, L. R.: Molecular insights on aging and aqueous-phase processing from ambient biomass burning emissions-influenced Po Valley fog and aerosol, Atmos. Chem. Phys., 18, 13197-13214, 10.5194/acp-18-13197-2018, 2018.

390

Chen, Y., Cao, J., Zhao, J., Xu, H., Arimoto, R., Wang, G., Han, Y., Shen, Z., and Li, G.: N-alkanes and polycyclic aromatic hydrocarbons in total suspended particulates from the southeastern Tibetan Plateau: concentrations, seasonal variations, and sources, Sci. Total. Environ., 470-471, 9-18, 10.1016/j.scitotenv.2013.09.033, 2014.

395 Chen, Y., Tian, M., Huang, R.-J., Shi, G., Wang, H., Peng, C., Cao, J., Wang, Q., Zhang, S., and Guo, D.: Characterization of urban amine-containing particles in southwestern China: seasonal variation, source, and processing, Atmos. Chem. Phys., 19, 2019.

Creamean, J. M., Lee, C., Hill, T. C., Ault, A. P., DeMott, P. J., White, A. B., Ralph, F. M., and Prather, K. A.: Chemical properties of insoluble precipitation residue particles, J. Aerosol. Sci., 76, 13-27, 10.1016/j.jaerosci.2014.05.005, 2014.

400 Darer, A. I., Cole-Filipiak, N. C., O'Connor, A. E., and Elrod, M. J.: Formation and stability of atmospherically relevant isoprene-derived organosulfates and organonitrates, Environ Sci Technol, 45, 1895-1902, 2011.

Dinar, E., Anttila, T., and Rudich, Y.: CCN activity and hygroscopic growth of organic aerosols following reactive uptake of ammonia, Environ Sci Technol, 42, 793-799, 2008.

Ditto, J. C., He, M., Hass-Mitchell, T. N., Moussa, S. G., Hayden, K., Li, S.-M., Liggio, J., Leithead, A., Lee, P., Wheeler, 405 M. J., Wentzell, J. J. B., and Gentner, D. R.: Atmospheric evolution of emissions from a boreal forest fire: the formation of highly functionalized oxygen-, nitrogen-, and sulfur-containing organic compounds, Atmos. Chem. Phys., 21, 255-267, 10.5194/acp-21-255-2021, 2021.

Ditto, J. C., Barnes, E. B., Khare, P., Takeuchi, M., Joo, T., Bui, A. A. T., Lee-Taylor, J., Eris, G., Chen, Y., Aumont, B., Jimenez, J. L., Ng, N. L., Griffin, R. J., and Gentner, D. R.: An omnipresent diversity and variability in the chemical 410 composition of atmospheric functionalized organic aerosol, Communications Chemistry, 1, 75, 10.1038/s42004-018-0074-3, 2018.

Ervens, B., Turpin, B. J., and Weber, R. J.: Secondary organic aerosol formation in cloud droplets and aqueous particles (aqSOA): a review of laboratory, field and model studies, Atmos. Chem. Phys., 11, 11069-11102, 10.5194/acp-11-11069-2011, 2011.

415 George, C., Ammann, M., D'Anna, B., Donaldson, D. J., and Nizkorodov, S. A.: Heterogeneous photochemistry in the atmosphere, Chem. Rev., 115, 4218-4258, 10.1021/cr500648z, 2015.

Hallquist, M., Wenger, J. C., Baltensperger, U., Rudich, Y., Simpson, D., Claeys, M., Dommen, J., Donahue, N. M., George, C., Goldstein, A. H., Hamilton, J. F., Herrmann, H., Hoffmann, T., Iinuma, Y., Jang, M., Jenkin, M. E., Jimenez, J. L., Kiendler-Scharr, A., Maenhaut, W., McFiggans, G., Mentel, T. F., Monod, A., Prevot, A. S. H., Seinfeld, J. H., Surratt, J. D.,
420 Szmigielski, R., and Wildt, J.: The formation, properties and impact of secondary organic aerosol: current and emerging issues, Atmos Chem Phys, 9, 5155-5236, 2009.

He, C., He, D., Chen, C., and Shi, Q.: Application of Fourier Transform Ion Cyclotron Resonance Mass Spectrometry in molecular characterization of dissolved organic matter, Science China: Earth Sciences, https://doi.org/10.1360/SSTe-2021-0390, 2022.

425 He, C., Fang, Z., Li, Y., Jiang, C., Zhao, S., Xu, C., Zhang, Y., and Shi, Q.: Ionization selectivity of electrospray and atmospheric pressure photoionization FT-ICR MS for petroleum refinery wastewater dissolved organic matter, Environmental Science: Processes & Impacts, 23, 1466-1475, 10.1039/d1em00248a, 2021a.

He, Q., Tomaz, S., Li, C., Zhu, M., Meidan, D., Riva, M., Laskin, A., Brown, S. S., George, C., Wang, X., and Rudich, Y.: Optical Properties of Secondary Organic Aerosol Produced by Nitrate Radical Oxidation of Biogenic Volatile Organic
430 Compounds, Environ. Sci. Technol., 55, 2878-2889, 10.1021/acs.est.0c06838, 2021b.

Hodshire, A. L., Akherati, A., Alvarado, M. J., Brown-Steiner, B., Jathar, S. H., Jimenez, J. L., Kreidenweis, S. M., Lonsdale, C. R., Onasch, T. B., Ortega, A. M., and Pierce, J. R.: Aging Effects on Biomass Burning Aerosol Mass and Composition: A Critical Review of Field and Laboratory Studies, Environ Sci Technol, 53, 10007-10022, 10.1021/acs.est.9b02588, 2019.

435 Huang, R. J., Zhang, Y., Bozzetti, C., Ho, K. F., Cao, J. J., Han, Y., Daellenbach, K. R., Slowik, J. G., Platt, S. M., Canonaco, F., Zotter, P., Wolf, R., Pieber, S. M., Bruns, E. A., Crippa, M., Ciarelli, G., Piazzalunga, A., Schwikowski, M., Abbaszade, G., Schnelle-Kreis, J., Zimmermann, R., An, Z., Szidat, S., Baltensperger, U., El Haddad, I., and Prevot, A. S.: High secondary aerosol contribution to particulate pollution during haze events in China, Nature, 514, 218-222, 10.1038/nature13774, 2014.

440 Jiang, B., Liang, Y., Xu, C., Zhang, J., Hu, M., and Shi, Q.: Polycyclic aromatic hydrocarbons (PAHs) in ambient aerosols from Beijing: characterization of low volatile PAHs by positive-ion atmospheric pressure photoionization (APPI) coupled with Fourier transform ion cyclotron resonance, Environ. Sci. Technol., 48, 4716-4723, 10.1021/es405295p, 2014.

Kanawati, B., Herrmann, F., Joniec, S., Winterhalter, R., and Moortgat, G. K.: Mass spectrometric characterization of beta-caryophyllene ozonolysis products in the aerosol studied using an electrospray triple quadrupole and time-of-flight analyzer

445 hybrid system and density functional theory, Rapid Commun. Mass. Spectrom., 22, 165-186, 10.1002/rcm.3340, 2008.

Koch, B. P. and Dittmar, T.: From mass to structure: an aromaticity index for high-resolution mass data of natural organic matter, **Rapid Commun. Mass. Spectrom.**, 20, 926-932, 10.1002/rcm.2386, 2006.

Kroll, J. H., Donahue, N. M., Jimenez, J. L., Kessler, S. H., Canagaratna, M. R., Wilson, K. R., Altieri, K. E., Mazzoleni, L. R., Wozniak, A. S., Bluhm, H., Mysak, E. R., Smith, J. D., Kolb, C. E., and Worsnop, D. R.: Carbon oxidation state as a

450 metric for describing the chemistry of atmospheric organic aerosol, Nat. Chem., 3, 133-139, 10.1038/nchem.948, 2011.

Kurek, M. R., Poulin, B. A., McKenna, A. M., and Spencer, R. G. M.: Deciphering Dissolved Organic Matter: Ionization, Dopant, and Fragmentation Insights via Fourier Transform-Ion Cyclotron Resonance Mass Spectrometry, Environ. Sci. Technol., 54, 16249-16259, 10.1021/acs.est.0c05206, 2020.

Laskin, J., Laskin, A., Nizkorodov, S. A., Roach, P., Eckert, P., Gilles, M. K., Wang, B., Lee, H. J., and Hu, Q.: Molecular

455 selectivity of brown carbon chromophores, Environ. Sci. Technol., 48, 12047-12055, 10.1021/es503432r, 2014.

Li, H., Zhang, Q., Zhang, Q., Chen, C., Wang, L., Wei, Z., Zhou, S., Parworth, C., Zheng, B., Canonaco, F., Prévôt, A. S. H., Chen, P., Zhang, H., Wallington, T. J., and He, K.: Wintertime aerosol chemistry and haze evolution in an extremely polluted city of the North China Plain: significant contribution from coal and biomass combustion, Atmos Chem Phys, 17, 4751-4768, 10.5194/acp-17-4751-2017, 2017a.

460 Li, K., Li, J., Liggio, J., Wang, W., Ge, M., Liu, Q., Guo, Y., Tong, S., Li, J., Peng, C., Jing, B., Wang, D., and Fu, P.: Enhanced Light Scattering of Secondary Organic Aerosols by Multiphase Reactions, Environ Sci Technol, 51, 1285-1292, 10.1021/acs.est.6b03229, 2017b.

Li, X., Yu, F., Cao, J., Fu, P., Hua, X., Chen, Q., Li, J., Guan, D., Tripathee, L., Chen, Q., and Wang, Y.: Chromophoric dissolved organic carbon cycle and its molecular compositions and optical properties in precipitation in the Guanzhong

465 basin, China, Sci. Total. Environ., 814, 152775, 10.1016/j.scitotenv.2021.152775, 2022.

Liggio, J. and Li, S.-M.: Organosulfate formation during the uptake of pinonaldehyde on acidic sulfate aerosols, Geophys Res Lett, 33, L13808-L13808, 10.1029/2006gl026079, 2006.

Lim, Y. B., Kim, H., Kim, J. Y., and Turpin, B. J.: Photochemical organonitrate formation in wet aerosols, Atmos. Chem. Phys., 16, 12631-12647, 10.5194/acp-16-12631-2016, 2016.

470 Lin, P., Rincon, A. G., Kalberer, M., and Yu, J. Z.: Elemental composition of HULIS in the Pearl River Delta Region, China: results inferred from positive and negative electrospray high resolution mass spectrometric data, Environ. Sci. Technol., 46, 7454-7462, 10.1021/es300285d, 2012.

Liu, Y., Liggio, J., Staebler, R., and Li, S. M.: Reactive uptake of ammonia to secondary organic aerosols: kinetics of organonitrogen formation, Atmos. Chem. Phys., 15, 13569-13584, 10.5194/acp-15-13569-2015, 2015a.

475 Liu, Y., Liggio, J., Staebler, R., and Li, S. M.: Reactive uptake of ammonia to secondary organic aerosols: kinetics of organonitrogen formation, Atmos. Chem. Phys., 15, 13569-13584, 10.5194/acp-15-13569-2015, 2015b.

McGuire, M. L., Chang, R. Y. W., Slowik, J. G., Jeong, C. H., Healy, R. M., Lu, G., Mihele, C., Abbatt, J. P. D., Brook, J. R., and Evans, G. J.: Enhancing non-refractory aerosol apportionment from an urban industrial site through receptor modelling of complete high time-resolution aerosol mass spectra, Atmos. Chem. Phys., 14, 5081-5145, 10.5194/acpd-14-
480 5081-2014, 2014.

Pöschl, U.: Atmospheric Aerosols: Composition, Transformation, Climate and Health Effects, Angewandte Chemie International Edition, 44, 7520-7540, doi:10.1002/anie.200501122, 2005.

Ray, D., Singh, S., Ghosh, S. K., and Raha, S.: Dynamic response of light absorption by PM2.5 bound water-soluble organic carbon to heterogeneous oxidation, Aerosol Sci. Technol., 53, 1404-1414, 10.1080/02786826.2019.1661350, 2019.

485 Rice, S., Maurer, D. L., Fennell, A., Dharmadhikari, M., and Koziel, J. A.: Evaluation of Volatile Metabolites Emitted In-Vivo from Cold-Hardy Grapes during Ripening Using SPME and GC-MS: A Proof-of-Concept, Molecules, 24, 536, 10.3390/molecules24030536, 2019.

Seidel, M., Beck, M., Riedel, T., Waska, H., Suryaputra, I. G. N. A., Schnetger, B., Niggemann, J., Simon, M., and Dittmar, T.: Biogeochemistry of dissolved organic matter in an anoxic intertidal creek bank, Geochim.Cosmochim. Acta, 140, 418-
490 434, 10.1016/j.gca.2014.05.038, 2014.

Seidel, M., Yager, P. L., Ward, N. D., Carpenter, E. J., Gomes, H. R., Krusche, A. V., Richey, J. E., Dittmar, T., and Medeiros, P. M.: Molecular-level changes of dissolved organic matter along the Amazon River-to-ocean continuum, Mar. Chem., 177, 218-231, 10.1016/j.marchem.2015.06.019, 2015.

Song, J., Li, M., Zou, C., Cao, T., Fan, X., Jiang, B., Yu, Z., Jia, W., and Peng, P.: Molecular Characterization of Nitrogen-Containing Compounds in Humic-like Substances Emitted from Biomass Burning and Coal Combustion, Environ. Sci. Technol., 56, 119-130, 10.1021/acs.est.1c04451, 2022.

Stenson, A. C., Marshall, A. G., and Cooper, W. T.: Exact masses and chemical formulas of individual Suwannee River fulvic acids from ultrahigh resolution electrospray ionization Fourier transform ion cyclotron resonance mass spectra, Anal Chem, 75, 1275-1284, 10.1021/ac026106p, 2003.

Tang, J., Li, J., Su, T., Han, Y., Mo, Y., Jiang, H., Cui, M., Jiang, B., Chen, Y., Tang, J., Song, J., Peng, P. a., and Zhang, G.: Molecular compositions and optical properties of dissolved brown carbon in biomass burning, coal combustion, and vehicle emission aerosols illuminated by excitation–emission matrix spectroscopy and Fourier transform ion cyclotron resonance mass spectrometry analysis, Atmos. Chem. Phys., 20, 2513-2532, 10.5194/acp-20-2513-2020, 2020.

Tao, J., Zhang, L., Cao, J., and Zhang, R.: A review of current knowledge concerning PM 2. 5 chemical composition, aerosol optical properties and their relationships across China, Atmos. Chem. Phys., 17, 9485-9518, 2017.

Wang, H., Qiao, B., Zhang, L., Yang, F., and Jiang, X.: Characteristics and sources of trace elements in PM2.5 in two megacities in Sichuan Basin of southwest China, Environ Pollut, 242, 1577-1586, 10.1016/j.envpol.2018.07.125, 2018.

Wang, Y., Hu, M., Lin, P., Tan, T., Li, M., Xu, N., Zheng, J., Du, Z., Qin, Y., Wu, Y., Lu, S., Song, Y., Wu, Z., Guo, S., Zeng, L., Huang, X., and He, L.: Enhancement in Particulate Organic Nitrogen and Light Absorption of Humic-Like Substances over Tibetan Plateau Due to Long-Range Transported Biomass Burning Emissions, Environ. Sci. Technol., 53, 14222-14232, 10.1021/acs.est.9b06152, 2019.

Xie, Q., Su, S., Chen, S., Xu, Y., Cao, D., Chen, J., Ren, L., Yue, S., Zhao, W., Sun, Y., Wang, Z., Tong, H., Su, H., Cheng, Y., Kawamura, K., Jiang, G., Liu, C.-Q., and Fu, P.: Molecular characterization of firework-related urban aerosols using Fourier transform ion cyclotron resonance mass spectrometry, Atmos. Chem. Phys., 20, 6803-6820, 10.5194/acp-20-6803-2020, 2020.

Yu, L., Smith, J., Laskin, A., George, K. M., Anastasio, C., Laskin, J., Dillner, A. M., and Zhang, Q.: Molecular transformations of phenolic SOA during photochemical aging in the aqueous phase: competition among oligomerization, functionalization, and fragmentation, Atmos Chem Phys, 16, 4511-4527, 10.5194/acp-16-4511-2016, 2016.

Yun, Y., Liang, L., Wei, Y., Luo, Z., Yuan, F., Li, G., and Sang, N.: Exposure to Nitro-PAHs interfere with germination and early growth of Hordeum vulgare via oxidative stress, Ecotoxicol. Environ. Saf., 180, 756-761, 10.1016/j.ecoenv.2019.05.032, 2019.

Zarzana, K. J., De Haan, D. O., Freedman, M. A., Hasenkopf, C. A., and Tolbert, M. A.: Optical Properties of the Products of α-Dicarbonyl and Amine Reactions in Simulated Cloud Droplets, Environ Sci Technol, 46, 4845-4851, 10.1021/es2040152, 2012.

Zhang, Q., Jimenez, J. L., Canagaratna, M. R., Ulbrich, I. M., Ng, N. L., Worsnop, D. R., and Sun, Y.: Understanding atmospheric organic aerosols via factor analysis of aerosol mass spectrometry: a review, Anal. Bioanal. Chem., 401, 3045-3067, 10.1007/s00216-011-5355-y, 2011.

Zhang, Q., Jimenez, J. L., Canagaratna, M. R., Allan, J. D., Coe, H., Ulbrich, I., Alfarra, M. R., Takami, A., Middlebrook, A. M., Sun, Y. L., Dzepina, K., Dunlea, E., Docherty, K., DeCarlo, P. F., Salcedo, D., Onasch, T., Jayne, J. T., Miyoshi, T., Shimono, A., Hatakeyama, S., Takegawa, N., Kondo, Y., Schneider, J., Drewnick, F., Borrmann, S., Weimer, S., Demerjian, K., Williams, P., Bower, K., Bahreini, R., Cottrell, L., Griffin, R. J., Rautiainen, J., Sun, J. Y., Zhang, Y. M., and Worsnop, D. R.: Ubiquity and dominance of oxygenated species in organic aerosols in anthropogenically-influenced Northern Hemisphere midlatitudes, Geophys. Res. Lett., 34, n/a-n/a, 10.1029/2007gl029979, 2007.

Zhang, R., Wang, G., Guo, S., Zamora, M. L., Ying, Q., Lin, Y., Wang, W., Hu, M., and Wang, Y.: Formation of urban fine particulate matter, Chem. Rev., 115, 3803-3855, 10.1021/acs.chemrev.5b00067, 2015.

Zhang, Z., Zhao, W., Hu, W., Deng, J., Ren, L., Wu, L., Chen, S., Meng, J., Pavuluri, C. M., Sun, Y., Wang, Z., Kawamura, K., and Fu, P.: Molecular characterization and spatial distribution of dicarboxylic acids and related compounds in fresh snow in China, Environ. Pollut., 291, 118114, 10.1016/j.envpol.2021.118114, 2021.